AAC
Journals.ASM.org

# Ocular Distribution, Spectrum of Activity, and *In Vivo* Viral Neutralization of a Fully Humanized Anti-Herpes Simplex Virus IgG Fab Fragment following Topical Application

**Marianne Berdugo,[a,b,c] Inna V. Larsen,[d,e] Claire Abadie,[f] Catherine Deloche,[f] Laura Kowalczuk,[a,b,c] Elodie Touchard,[a,b,c] Richard Dubielzig,[e,g] Curtis R. Brandt,[d,e,h] Francine Behar-Cohen,[a,b,c,i] and Jean-Marc Combette[f]**

INSERM, UMR S 872, Les Cordeliers, Paris, France[a]; Université Pierre et Marie Curie-Paris 6, UMR S 872, Paris, France[b]; Université Paris Descartes, UMR S 872, Paris, France[c]; Department of Ophthalmology and Visual Sciences, University of Wisconsin School of Medicine and Public Health, Madison, Wisconsin, USA[d]; Collaborative Ocular Research Laboratories (CORL), University of Wisconsin—Madison, Madison, Wisconsin, USA[e]; Solid Drug Development, Geneva, Switzerland[f]; Department of Surgical Sciences, School of Veterinary Medicine, University of Wisconsin—Madison, Madison, Wisconsin, USA[g]; Department of Medical Microbiology and Immunology, University of Wisconsin School of Medicine and Public Health, Madison, Wisconsin, USA[h]; and Hotel-Dieu University Hospital of Paris, Paris, France[i]

**Herpes simplex ocular infection is a major cause of corneal blindness. Local antiviral treatments exist but are associated with corneal toxicity, and resistance has become an issue. We evaluated the biodistribution and efficacy of a humanized anti-herpes simplex virus (anti-HSV) IgG FAb fragment (AC-8; 53 kDa) following repeated topical administration. AC-8 was found in the corneal epithelium, anterior stroma, subepithelial stromal cells, and retinal glial cells, with preferential entry through the ocular limbus. AC-8 was active against 13 different strains of HSV-1, with 50% and 90% mean effective concentrations ($MEC_{50}$ and $MEC_{90}$, respectively) ranging from 0.03 to 0.13 $\mu$g/ml, indicating broad-spectrum activity. The *in vivo* efficacy of AC-8 was evaluated in a mouse model of herpes-induced ocular disease. Treatment with low-dose AC-8 (1 mg/ml) slightly reduced the ocular disease scores. A greater reduction of the disease scores was observed in the 10-mg/ml AC-8-treated group, but not as much as with trifluridine (TFT). AC-8 treatment reduced viral titers but less than trifluridine. AC-8 did not display any toxicity to the cornea or other structures in the eye. In summary, topical instillation of an anti-HSV FAb can be used on both intact and ulcerated corneas. It is well tolerated and does not alter reepithelialization. Further studies to improve the antiviral effect are needed for AC-8 to be considered for therapeutic use.**

Herpes simplex virus (HSV) ocular infection is the leading cause of infectious corneal blindness in the United States. Although trifluridine (or trifluorthymidine) (TFT) is approved for therapy, there are challenges such as toxicity and the development of resistant strains of virus. Monoclonal antibodies or other protein-based therapies have significant potential for treating ocular disease in humans. For example, ranibizumab, a monoclonal Fab fragment directed against vascular endothelial growth factor (VEGF), was recently approved by the FDA for the treatment of wet age-related macular degeneration but requires repeated intravitreal injections. Other monoclonal antibodies have been used to neutralize cytokines or proangiogenic compounds after intravenous (i.v.) or intravitreal administration (18). The main advantage of monoclonal antibodies is their specificity of action. However, due to their molecular weight, intraocular injection is the only local route currently used in clinical practice. Topical routes of administration are less invasive than intraocular injections. Proteins or peptides are typically not delivered by topical instillation since it is generally thought that they do not penetrate the eye via this route. However, insulin (8 kDa), combined with a penetration enhancer, was found in the retina at low levels and seemed to accumulate in the optic nerve after instillation (11). Nerve growth factor (NGF; 26 kDa) was also found in the retina and optic nerve after topical instillation, but no NGF was found in the corneal stroma, suggesting a trans-scleral pathway was favored over direct transcorneal penetration (12). A single-chain variable domain antibody fragment (28 kDa) could be detected in the vitreous at therapeutic levels if topically applied frequently (24). We have recently shown that ESBA105 (an anti-tumor necrosis factor alpha [anti-TNF-$\alpha$] single-chain antibody of 26 kDa) can reach the retina and all ocular compartments after topical administration without any penetration enhancer. Systemic exposure after topical administration was 25,000-fold lower than exposure after i.v. injection of the identical cumulative daily dose. ESBA105 levels in vitreous humor and neuroretina were significantly higher after topical administration than after i.v. injection. The kinetics profile also suggested a trans-scleral pathway (6).

Monoclonal antibodies can also be used to specifically neutralize infectious agents, including herpes simplex virus (HSV) (19). Monoclonal antibodies or their Fab fragments to HSV glycoprotein D (gD) have been used topically to prevent vaginal transmission of HSV-2 (25, 26). Interestingly, topical antibodies have protected from HSV infection for more than 24 h (26). Moreover, after HSV-1 corneal infection in mice, a human monoclonal antibody directed against HSV was found in infected corneal nerve fibers after repeated intraperitoneal injections, suggesting that it could interfere with virus spread (20).

**Received** 27 June 2011 **Returned for modification** 11 August 2011
**Accepted** 19 December 2011
**Published ahead of print** 27 December 2011
Address correspondence to F. Behar-Cohen, francine.behar@gmail.com.
F. Behar-Cohen and J.-M. Combette contributed equally to this article.
Supplemental material for this article may be found at http://aac.asm.org/.

doi:10.1128/AAC.05145-11

*AC-8 heavy chain sequence:*

```
          10          20          30          40          50          60
QVQLVQSGAE VKKPGSSVKV SCKASGGSFS SYAINWVRQA PGQGLEWMGG LMPIFGTTNY
          70          80          90         100         110         120
AQKFQDRLTI TADVSTSTAY MQLSGLTYED TAMYYCARVA YMLEPTVTAG GLDVWGQGTT
         130         140         150         160         170         180
VTVSSASTKG PSVFPLAPSS KSTSGGTAAL GCLVKDYFPE PVTVSWNSGA LTSGVHTFPA
         190         200         210         220         230
VLQSSGLYSL SSVVTVPSSS LGTQTYICNV NHKPSNTKVD KKVEPKSCDK T

Number of amino acids: 231

Theoretical Molecular weight: 24242.3

Theoretical pI: 8.75

>AC8-HC

QVQLVQSGAEVKKPGSSVKVSCKASGGSFSSYAINWVRQAPGQGLEWMGGLMPIFGTTNY
AQKFQDRLTITADVSTSTAYMQLSGLTYEDTAMYYCARVAYMLEPTVTAGGLDVWGQGTT
VTVSSASTKGPSVFPLAPSSKSTSGGTAALGCLVKDYFPEPVTVSWNSGALTSGVHTFPA
VLQSSGLYSLSSVVTVPSSSLGTQTYICNVNHKPSNTKVDKKVEPKSCDKT
```

*AC-8 light chain sequence:*

```
          10          20          30          40          50          60
EIVLTQSPGT LSLSPGERAT LSCRASQSVS SAYLAWYQQK PGQAPRLLIY GASSRATGIP
          70          80          90         100         110         120
DRFSGSGSGT DFTLTISRLE PEDFAVYYCQ QYGRSPTFGG GTKVEIKRTV AAPSVFIFPP
         130         140         150         160         170         180
SDEQLKSGTA SVVCLLNNFY PREAKVQWKV DNALQSGNSQ ASVTEQDSKD STYSLSSTLT
         190         200         210
LSKADYEKHK VYACEVTHQG LSSPVTKSFN RGEC

Number of amino acids: 214

Theoretical Molecular weight: 23220.8

Theoretical pI: 7.83

>AC8-LC

EIVLTQSPGTLSLSPGERATLSCRASQSVSSAYLAWYQQKPGQAPRLLIYGASSRATGIP
DRFSGSGSGTDFTLTISRLEPEDFAVYYCQQYGRSPTFGGGTKVEIKRTVAAPSVFIFPP
SDEQLKSGTASVVCLLNNFYPREAKVQWKVDNALQSGNSQASVTEQDSKDSTYSLSSTLT
LSKADYEKHKVYACEVTHQGLSSPVTKSFNRGEC
```

**FIG 1** Heavy chain (HC) and light chain (LC) sequences of the tested Fab fragment named AC-8.

The aim of this study was to evaluate the ocular penetration and distribution of a fully humanized IgG Fab fragment (AC-8) designed to neutralize HSV-1 and HSV-2 after topical instillation without permeation enhancer, to determine the spectrum of activity of AC-8 against 13 ocular HSV isolates, and to evaluate its efficacy in an HSV-1 strain KOS-induced mouse model of ocular disease.

## MATERIALS AND METHODS

**AC-8.** AC-8 is a Fab fragment (53 kDa) of a fully humanized antibody specific for glycoprotein D (gD) of both HSV-1 and HSV-2, as described by Burioni et al. (4). AC-8 heavy and light chains (AC8-HC and AC8-LC, respectively) were constructed as presented in Fig. 1. The AC-8 Fab fragment was classified as subgroup Ib on the basis of gD truncation recognition (5).

A scrambled sequence of AC-8 (termed "Fab fragment" in this study) was used as a negative control and was constructed as presented in Fig. 2. The scrambled nonbinding AC8-HC fragment was created by rearranging the amino acid residues of the CDR3 region (Fig. 2A). This mutant (Sc) is used as a negative control. A comparison of both AC8-HC fragments is presented in Fig. 2B.

For topical and subconjunctival administrations, AC-8 was diluted in 1× phosphate-buffered saline (PBS) (pH 7; osmolarity, 330 mmol/liter; stored at 4°C). The volume delivered for each topical drop and subconjunctival injection in rats was 50 $\mu$l.

**AC-8 administration, quantification, and distribution to normal and de-epithelialized rat eyes.** Six- to 8-week-old Albino Lewis male rats (Elevage Charles River, L'Arbresle, France), each weighing 120 to 150 g, were used in the immunohistochemistry part of the study, and 8-week-old Brown Norway pigmented rats, each weighing 150 to 200 g, were used for the enzyme-linked immunosorbent assay (ELISA) AC-8 quantification (Elevage Charles River, L'Arbresle, France). The reason for using two different rat strains was that pigmented rats are more relevant as animal models of human pathologies, whereas albino rats have reduced immunohistochemical autofluorescence of ocular tissues. All experiments were conducted in accordance with the ARVO "Statement for the Use of Animals in Ophthalmic and Vision Research" (www.arvo.org). During surgical procedures and subconjunctival injections, rats received intramuscular injections for general anesthesia (88 mg/kg body weight ketamine [ketamine 1000; Virbac, Carros, France] plus 0.6 mg/kg body weight chlorpromazine [Largactil; Sanofi-Aventis, Paris, France]), and local anesthesia was obtained with topical oxybuprocaine 0.4% (Novésine; Merck Sharp & Dohme-Chibret, Paris, France). For topical administration, rats were gently restrained without anesthesia and held still for 20 s to allow drop penetration of the eye. At the end of the experiments, the animals were sacrificed by intraperitoneal injection of a lethal dose of pentobarbital (750 mg/kg body weight [Pentobarbital Sodique; Ceba Santé Animale, Libourne, France]).

**Ulcerative keratopathy model.** At day 0, rats were anesthetized and the right cornea of each rat underwent de-epithelialization using a calibrated 3-mm biopsy punch (Stiefel Laboratories, Coral Gables, FL) and a surgical crescent knife (Alcon, Fort Worth, TX). The left eye of each rat was left untreated as a control.

**Topical and subconjunctival administration of AC-8.** Three sets of experiments were carried out to evaluate the penetration of the AC-8 Fab fragment that was topically administered onto normal (experiment 1) or de-epithelialized corneas (experiments 2 and 3). Experiments 2 and 3 evaluated the biodistribution of AC-8 in de-epithelialized rat corneas and during the re-epithelialization period, mimicking a corneal ulcer. AC-8 was administered at 10 $\mu$g/ml in experiment 1, 100 $\mu$g/ml in experiment 2, and 1,000 $\mu$g/ml in experiment 3. PBS was used as the vehicle control.

In experiment 1 (3 rats per group), group 1 received a single instillation of AC-8, and the rats were sacrificed 1 h later. Group 2 received one drop of AC-8 per hour for 5 consecutive hours, and the rats were sacrificed 1 h after the last instillation. Group 3 received 5 instillations of AC-8 per day (from 8:00 a.m. to 9:00 p.m.) from day 0 to day 3, and the rats were sacrificed 1 h after the first drop on day 4. Groups 4 and 5 were treated with a single subconjunctival injection of AC-8, and the rats were sacrificed 1 and 6 h after the injection, respectively. Group 6 received 5 instillations of vehicle per day (from 8:00 a.m. to 9:00 p.m.) from day 0 to day 3, and the rats were sacrificed 1 h after the first instillation on day 4. Group 7 received one subconjunctival injection of vehicle, and the rats were sacrificed 1 h later.

In experiment 2 (3 rats per group), groups 1 and 2 were treated with AC-8 5 times on day 0, and the rats were sacrificed 1 h and 24 h later, respectively. Group 3 received AC-8 5 times per day on day 0 and day 1, and the rats were sacrificed 1 h after one instillation on day 2. Groups 4, 5, and 6 received a single subconjunctival injection of AC-8, and the rats were sacrificed 1, 6, and 24 h posttreatment, respectively. Group 7 received 5 instillations of vehicle per day on days 0 and 1, and the rats were sacrificed 1 h after one instillation of vehicle on day 2. Group 8 was treated with one subconjunctival injection of vehicle, and the rats were sacrificed 1 h later.

Experiment 3 was performed to quantify AC-8 after instillation or

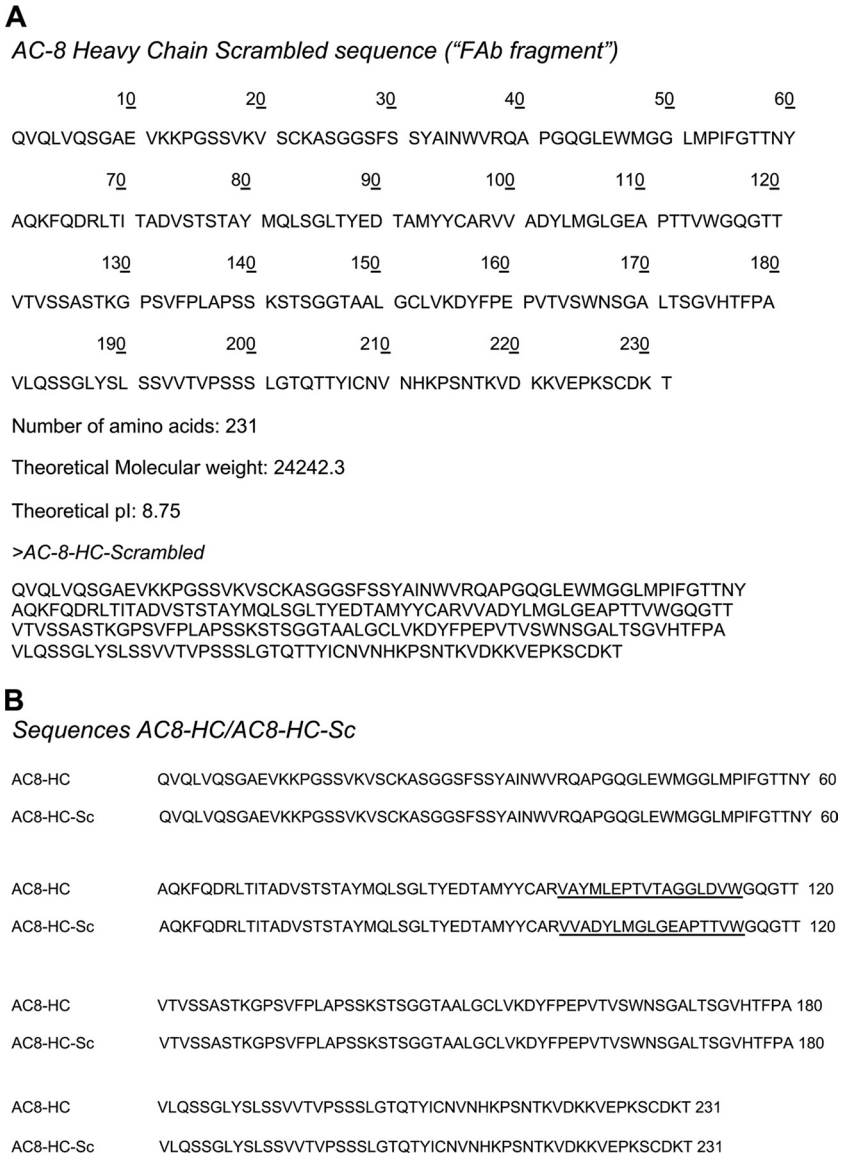


**FIG 2** Heavy chain (HC) scrambled (Sc) sequence of the Fab fragment used as a negative control (A). Heavy chain sequences show comparison between AC-8 and scrambled AC-8 (B).

subconjunctival injection. Since a preliminary study showed that using 10 $\mu$g/ml AC-8 was below detectable levels in the ocular tissues, we used 1 mg/ml AC-8 in PBS. At this concentration, AC-8 was stable in solution. Rats (6 per time point) were treated by topical instillation 5 times a day and sacrificed 1, 6, and 24 h posttreatment. Three other groups of rats were treated with a subconjunctival injection of AC-8 and sacrificed 1, 6, and 24 h posttreatment (6 rats per time point).

**Tissue preparation.** For experiments 1 and 2, eyes from each group were dissected and mounted in optimal cutting temperature (OCT) compound (Tissue-Tek; Sakura Finetek, Zoeterwoude, Netherlands) at −80°C for cryosectioning. For experiment 3, aqueous humors (approximately 10 to 20 $\mu$l per eye) and vitreous humors (approximately 20 to 30 $\mu$l per eye) were collected in Eppendorf tubes and stored at −80°C. Serum samples (approximately 1 to 2 ml per animal) were taken just before sacrifice and stored at −80°C. The corneal epithelium was separated from the stroma/endothelium, and the retina was separated. The tissues were snap-frozen for ELISA quantification.

**Immunofluorescence.** The frozen cryosections (10 $\mu$m thick) were fixed for 15 min in 4% paraformaldehyde, rinsed twice for 10 min in 1× PBS, and rinsed twice for 10 min in 0.1% Triton X-100 (in 1× PBS). They were incubated overnight at +4°C with a 1/50 dilution of goat anti-human IgG (31132; Pierce, Rockford, IL) in 1× PBS–0.1% Triton X-100. After overnight incubation, the samples were rinsed 3 times for 10 min in 1× PBS–0.1% Triton X-100, incubated for 1 h at +20°C in the dark with a 1/50 dilution of Alexa Fluor 594-labeled donkey anti-goat IgG (H+L) (Molecular Probes-Invitrogen, Cergy-Pontoise, France), rinsed twice for 10 min in 1× PBS, and incubated for 5 min in a 1/5,000 dilution of (4′,6′-diamidino-2-phenylindole) (DAPI; Sigma-Aldrich, Munich, Germany) in the dark. The sections were then rinsed 5 times for 5 min in 1× PBS and once for 5 min in distilled water, dried, and placed on microscope slides in Gel/Mount (Biomeda Corp., Foster City, CA). The slides were observed under a fluorescence microscope (BX51; Olympus, Rungis, France).

**ELISA quantification of AC-8 in ocular tissues and fluids.** Serum, aqueous and vitreous humors, and tissue analyses were performed using a sandwich ELISA. Anti-human Fab 122 fragment-specific antibody purified from goat [goat anti-human F(ab) 31132; Perbio, Pierce, Rockford, IL] was bound to the wells of a polystyrene microwell plate. Diluted rat

ocular matrices (e.g., aqueous humor or vitreous or ocular tissue) and sera were added to separate wells and incubated for 1 h at room temperature to allow AC-8 to bind to the immobilized antibody. The wells were then rinsed with PBS, and an enzyme-labeled (horseradish peroxidase [HRP]-conjugated) anti-human antibody (HRP-Fab goat anti-human IgG 109-036-097; Jackson ImmunoResearch, Interchim, Montluçon, France) was added to each well. After incubation for 1 h at room temperature, the wells were rinsed with PBS, chromogenic substrate (3,3′,5,5′-tetramethylbenzidine [TMB] substrate 34022; Perbio, Pierce, Rockford, IL) was added, and absorbance at 450 nm was measured using an automated microplate reader (ELX808IU series 188640; Biotek). The detection limits for the assay were 0.19 ng/mg of cornea, 0.106 ng/mg of retina, 27.8 ng/ml of aqueous humor, and 55.6 ng/ml of vitreous humor or serum.

**Spectrum of activity against ocular HSV isolates. (i) Cells.** African green monkey kidney (Vero) cells were grown in Dulbecco's modified Eagle's medium (DMEM [10-017-CM, Mediatech/Cellgro, Manassas, VA]) supplemented with either 5% serum for propagation (2.5% fetal bovine serum [FBS] [S11150; Atlanta Biologicals, Atlanta GA]–2.5% bovine calf serum [BCS] [SH30072.03; HyClone, Ogden, UT]) or 2% serum for viral infections (1% of each). The media were also supplemented with 10 ml/liter of penicillin-streptomycin (100 U/ml penicillin, 100 $\mu$g/ml streptomycin sulfate [G1146; Sigma/Aldrich, St. Louis, MO]) and 10 ml/liter of 250 $\mu$g/ml amphotericin B (30-003CF [Mediatech/Cellgro, Manassas, VA] or BP264520 [Fisher Scientific, Fair Lawn, NJ]). Cell cultures were grown at 37°C in an atmosphere of 5% $CO_2$.

**(ii) Viruses.** The laboratory strains HSV-1 KOS and F (ATCCVR-733) and the clinical ocular HSV-1 isolates CJ134, CJ394, CJ311, CJ411, CJ455, CJ462, CJ505, CJ515, CJ970, CJ994, and TFT 401 were tested (7). The clinical isolates were provided by John Chandler and were obtained in the Seattle, WA, area. Viral stocks were prepared as described previously (7). Briefly, high-titer stocks were prepared by infecting Vero cells at a multiplicity of infection (MOI) of 0.1, and harvesting each monolayer when the cytopathic effect was 90 to 100%. The infected cells were subjected to 3 freeze-thaw cycles using a dry ice-ethanol bath and centrifuged twice at 2,000 $\times$ *g* for 10 min at 4°C to remove debris. The samples were frozen at −80°C. The supernatant from the crude preparation was layered on a cushion of 36% sucrose in reaction stop buffer (RSB) (10 mM Tris HCl [pH 7.4], 10 mM NaCl, 3 mM $MgCl_2$) and centrifuged at 13,500 $\times$ *g* for 80 min at 10°C to pellet the virions (23). The pellet was then resuspended in RSB and stored at −80°C. The sucrose cushion step was repeated, and the pellets were resuspended in RSB and stored at −80°C. Viral titers were determined by plaque assay on Vero cell monolayers.

**(iii) Yield reduction assay.** Vero cells were plated on 24-well plates containing 1.4 $\times$ $10^5$ cells per well. AC-8 and control Fab compounds were serially diluted to yield final concentrations of 5, 2.5, 0.625, 0.3125, 0.156, and 0.078 $\mu$g/ml in DMEM containing 2% serum. The stock solution of TFT (10 mg/ml) was serially diluted to 2.5, 0.625, 0.3125, 0.156, 0.078, and 0.39 $\mu$g/ml in DMEM (2% serum) when mixed with virus. Each viral stock was diluted to a concentration of 1.4 $\times$ $10^6$ PFU/ml (MOI of 1.0) in DMEM with 2% serum. One hundred microliters of virus was mixed with either no drug or 100 $\mu$l of each dilution of the compound, added to the monolayers (50 $\mu$l per well), and incubated at 37°C for 1 h. Samples were prepared in triplicate. The medium was then aspirated, and the cells were refed with 400 $\mu$l of medium containing the desired concentration of AC-8. Control wells received medium only. The plate was incubated at 37°C for 18 to 24 h. The plate was then subjected to three freeze-thaw cycles (−80°C and +37°C). The contents of each well were transferred to microcentrifuge tubes and centrifuged at 2,000 $\times$ g for 10 min at room temperature. The supernatants were collected and serially diluted, and virus was quantitated by plaque assay on Vero cell monolayers in 6-well plates (7).

**(iv) $MEC_{50}$ and $MEC_{90}$ determination.** The mean effective concentrations required to reduce viral yields by 50% or 90% for each viral strain ($MEC_{50}$ and $MEC_{90}$, respectively) were determined from the yield reduction curves by counting the number of plaques present at each concentration of AC-8. The MEC value for each repeat (triplicates were analyzed) was used for the calculations. Fifty and 90 percent inhibition values were determined from the line graphs obtained for each test compound. Significant differences were analyzed by analysis of variance (ANOVA).

**Mouse inoculation and treatment. (i) Animals, viral inoculation, and treatments.** Eight-week-old female BALB/c mice (Harlan Sprague-Dawley, Indianapolis; IN) were used for this study. All treatment groups consisted of 10 mice each. Mice were randomly assigned to each treatment group, and each animal was weighed to obtain an average weight for dosing of ketamine, xylazine, and buprenorphine. Mice were anesthetized with a combination of 80-mg/kg ketamine (100 mg/ml 200-055; Lloyds Labs, Shenandoah, IA) and 5-mg/kg xylazine (100 mg/ml 139-236; Lloyds Labs, Shenandoah, IA). The right cornea was scarified with a sterile 30-gauge needle. Four scratches were made on the periphery parallel and as close to the corneo-scleral junction as possible. A 5-$\mu$l drop of DMEM (2% serum) containing 1.0 $\times$ $10^5$ PFU of HSV-1 KOS was applied to the scarified cornea. The eyelids were closed two times over the cornea, and the animals were returned to their cages. Treatment began within 2 to 4 h of infection (day 0) and continued for 8 days (days 1 through 8).

The following treatment arms were included: group 1, 1% trifluridine (61314-044-75; Alcon, Houston, TX); group 2, 1 mg/ml AC-8 in PBS (ribOvax, Geneva, Switzerland); group 3, 10 mg/ml AC-8 in PBS (ribOvax, Geneva, Switzerland); group 4, 10 mg/ml control Fab fragment in PBS (ribOvax, Geneva, Switzerland); group 5, PBS (pH 7.0) vehicle (ribOvax, Geneva, Switzerland). Trifluridine (TFT) was chosen as the control because it is licensed for ocular treatment of herpetic keratitis in the United States. All solutions were aliquoted and frozen at the start of the study. One vial was then thawed daily and stored at 4°C for the duration of that day's treatment. The animals were dosed at 2-h intervals, beginning at 8:00 a.m. and ending at 10:00 p.m. For each dosing, the mice were anesthetized with isoflurane (3 to 5%) (57319-47406; Phoenix Pharmaceutical, St. Joseph, MO), a 3-$\mu$l drop of the compound was administered to the infected eye, and the animals were returned to their cages. For comfort and analgesia, the mice were injected intraperitoneally with 0.01 mg/kg of buprenorphine (0.3 mg/ml 0409-20132; Hospira, Lake Forest, IL) twice a day (a.m. and p.m.) on days 0 through 8.

**(ii) Clinical disease scoring.** The severity of ocular disease was scored as previously described and is shown in Table 1 (3). To score epithelial keratitis, the corneas were stained by adding a drop of 1% fluorescein (Ful-Glo strips; Akorn, Inc., Buffalo Grove, IL) in PBS, followed by a PBS rinse, and illuminated using a cobalt blue light source (Wild Leitz, Jeer Heerbrugg, Switzerland).

Animals were scored at baseline (1 week after arrival and just before corneal scarification and virus inoculation); any animals showing corneal defects were excluded from the study. Subsequently, the mice were anesthetized with isoflurane (3 to 5%) and scored on odd days for 11 days (epithelial keratitis) or 15 days (blepharitis, corneal vascularization, and corneal opacity). All animal experiments were approved by the UW-Madison Institutional Animal Care and Use Committee and conformed to the "ARVO Statement for the Use of Animals in Ophthalmic and Vision Research."

**(iii) Measurement of tear film viral titers.** At the beginning of each day and prior to treatment, the animals were anesthetized with isoflurane and the infected cornea was flushed with 10 $\mu$l of DMEM containing 2% serum. The tear film contents were added to 190 $\mu$l of media and stored at −80°C. Tear film samples were collected from the mice on odd days through day 13, and titers were determined by standard plaque assay on Vero cell monolayers in 6-well plates.

**(iv) Statistical analysis.** All statistical analyses were done by the Biostatistic and Research Ethics Core—UW Institute for Clinical and Translational Research (ICTR). The Wilcoxon signed-rank test utilizing R statistical software was used. The significance threshold of the *P* value (0.05)

**TABLE 1** Clinical scoring system used in this study

| Clinical symptom | Characteristic(s) with clinical disease score of: | | | | |
|---|---|---|---|---|---|
| | 0 | 1+ | 2+ | 3+ | 4+ |
| Blepharitis | None | Noticeably puffy eyelids | Puffy eyelids with moderate crusting | Eye 50% swollen shut with moderate crusting | Eye completely swollen shut with severe crusting |
| Corneal neovascularization | None | <25% of the cornea involved | 25–50% involved | >50% of the cornea involved | |
| Stromal keratitis | None | Cloudiness, some iris detail visible | Iris detail obscured | Cornea totally opaque | Cornea perforated |
| Epithelial keratitis | None, corneal scratch (CS)[a] only | <25% of epithelium outside of CS stained | 50% of epithelium outside of CS stained | 50–75% of epithelium outside of CS stained | 75–100% of epithelium outside of CS stained |

[a] Cs, corneal scarification.

was adjusted by the number of pairwise comparisons between groups (raw disease scores, mean peak disease scores, and tear film titers) (10). Unpaired two-way *t* tests were run on the $MEC_{50}/MEC_{90}$ value data, and the *P* value was adjusted by 3 pairwise comparisons with the adjusted *P* values of 0.0033 and 0.0167, respectively.

**(v) Euthanasia and histology.** All animals were sacrificed on day 15 of the study, and the infected eyes were harvested and placed in 4% paraformaldehyde (P6148; Sigma, St. Louis, MO) in PBS. Two untreated and uninfected left eyes from each treatment group were also harvested. All eyes were embedded in paraffin, sectioned (5 $\mu$m each) along the pupil-optic nerve axis, and stained with hematoxylin and eosin (H&E) (Newcomer Supply, Middleton, WI). Sections were then examined for evidence of corneal edema, structural damage, cellular infiltration, and evidence of vascularization. The following histological parameters were scored (0 to 4) in each histological section: ulceration, uveitis, corneal neovascularization, lymphocytes in the cornea, neutrophils in the cornea, and neutrophils in the anterior chamber. The mean scores for each parameter and in each treatment group were compared.

## RESULTS

**AC-8 penetrates ocular tissues after repeated instillation.** No AC-8 was detected in the ocular tissues 1 h after a single topical instillation of 100 $\mu$g/ml AC-8 (data not shown). One hour after AC-8 was instilled 5 times per day, AC-8 could be detected at the periphery of the cornea. It was primarily located in the subepithelial cells and appeared as dots, which may correspond to engulfment by dendritic cells. In the ciliary body and the retina, a diffuse staining was detected compared to the PBS-treated rats (data not shown). However, after 4 days of AC-8 treatment (10 $\mu$g/ml) 5 times a day, followed by a single instillation on day 4, intense AC-8 staining was observed at the periphery (Fig. 3 d to f) as well as in the center (Fig. 3a to c) of the anterior corneal stroma. No signal was found in vehicle-treated eyes (Fig. 3j to l). AC-8 immunostaining was more intense in the limbus and in the ciliary body than at the center of the cornea, suggesting that AC-8 penetrated the eye through a transscleral pathway and secondarily diffused into the cornea. Staining of the corneal epithelium was more pronounced at the periphery (Fig. 3e and f) than at the center (Fig. 3b and c) of the cornea. Again, cells located mostly in the anterior stroma seem to have engulfed AC-8 (Fig. 3c, high-magnification inset).

In the retina, AC-8 immunoreactivity was found in astrocytes at the inner retinal border (Fig. 4a to d; arrowheads in panels b and c) and as a diffuse signal in all retinal layers, compared to the vehicle-treated control retina (Fig. 4e to g). For rats from group 3, who received 5 instillations per day for 4 days and were sacrificed 1 h after the first instillation on day 4, intraocular penetration was not different from that in rats from group 1, suggesting that the half-life of AC-8 was probably short and that no accumulation of AC-8 occurred.

The repeated instillations did not cause gross visible ocular damage, suggesting the ocular toxicity of AC-8 for eye tissues is low. Among all of the examined sections, we did not find any detectable histological damage resulting from AC-8 instillation, supporting the conclusion that AC-8 has little or no toxicity.

**Subconjunctival injection allows efficient penetration of AC-8 into tissues of the anterior and posterior segments.** One hour after a single subconjunctival injection of AC-8 (10 $\mu$g/ml), we observed very strong staining of both the anterior and the posterior segments of the eye compared to the vehicle-injected eyes (Fig. 5d to f for the cornea, j to l for the ciliary body, and p to r for the retina). In the cornea (Fig. 5a to c), diffuse AC-8 staining was found in the epithelium and in the stroma as well as in stromal cells (Fig. 5a to c; arrows in panels b and c). In the ciliary body (Fig. 5g to i), AC-8 accumulated in nonpigmented ciliary epithelial cells (Fig. 5h and i). In the retina (Fig. 5m to o and s and t), AC-8 was clearly located in astrocytes (Fig. 5s, arrowheads) and Müller cells (Fig. 5s, arrows). In the retinal pigment epithelial (RPE) cells, a strong signal was also observed (Fig. 5t).

Six hours posttreatment, low AC-8 immunoreactivity was observed in the corneal epithelium, but immunoreactivity remained essentially the same in the stroma, the limbus, and the ciliary body. No signal could be detected in the retina 6 h posttreatment (not shown). Twenty-four hours posttreatment, no difference was observed between AC-8- and vehicle-treated eyes.

**Enhanced intraocular penetration of AC-8 after topical instillation on de-epithelialized cornea.** All corneas in both AC-8-treated and control groups were re-epithelialized after 48 h, demonstrating that AC-8 did not influence the corneal epithelium healing process. While no intracorneal penetration of AC-8 was observed 1 h following the last of 5 daily instillations (10 $\mu$g/ml), AC-8 was found in the corneal stroma when the central epithelium was removed. AC-8 accumulated at the border of the ulcer (Fig. 6a to c) and in the anterior stroma of the peripheral (still epithelialized) cornea (Fig. 6d to f; arrows in panel e). In the iris and ciliary body, AC-8 could also be detected (Fig. 6g to j; arrows in panels h to j [j is high magnification of i]). No signal was found in the vehicle-treated eyes (not shown). In the limbus, AC-8 was found in cells located in the subepithelial space (Fig. 6h to j, arrows). Six and 24 h posttreatment, AC-8 could still be detected in

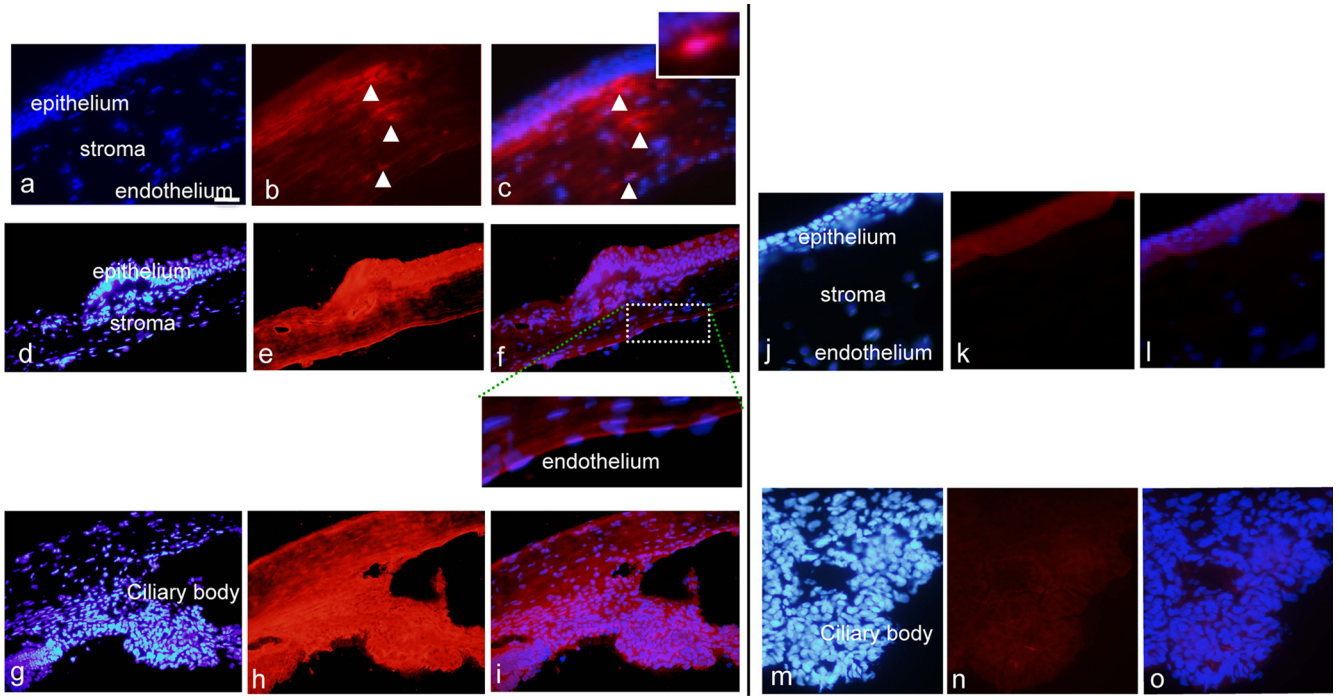


**FIG 3** Immunohistochemical analysis of the cornea and ciliary body of rats. Panels a to f show results 1 h after 5 instillations a day of 10 $\mu$g/ml AC-8 for 4 days and then a single instillation on day 4 (group 3; a to c, central cornea, and d to f, peripheral cornea). Insets show higher magnifications. Panels j to l show results 1 h after 5 instillations a day of PBS over 4 days and then a single instillation on day 4 (vehicle; group 6, j to l). Panels g to i show ciliary body with the same AC-8 treatment (group 3). Panels m to o show control PBS-treated ciliary body (group 6). Left panels show DAPI staining (blue), middle panels show Alexa-labeled anti human IgG antibody (red), and right panels show the merged images. Positively stained dendritiform subepithelial cells are indicated by arrowheads. Bar, 50 $\mu$m.

the cornea, the iris/ciliary body, and, to a lesser extent, the retina (data not shown).

In rats that received AC-8 5 times on day 0 and day 1 and were sacrificed 1 h after one instillation on day 2, AC-8 penetration was enhanced in the corneal epithelium (Fig. 7a to c) compared to vehicle-treated eyes. The AC-8 was particularly concentrated in the newly formed epithelium (Fig. 7a to c, dashed white squares) and in subepithelial stromal cells (Fig. 7b and c, arrows). No signal was found in the vehicle-treated eyes (Fig. 7d to f). In the retina, AC-8 was still present in retinal layers at the periphery of the retina (data not shown).

AC-8 biodistribution in corneas of mice infected by HSV-1

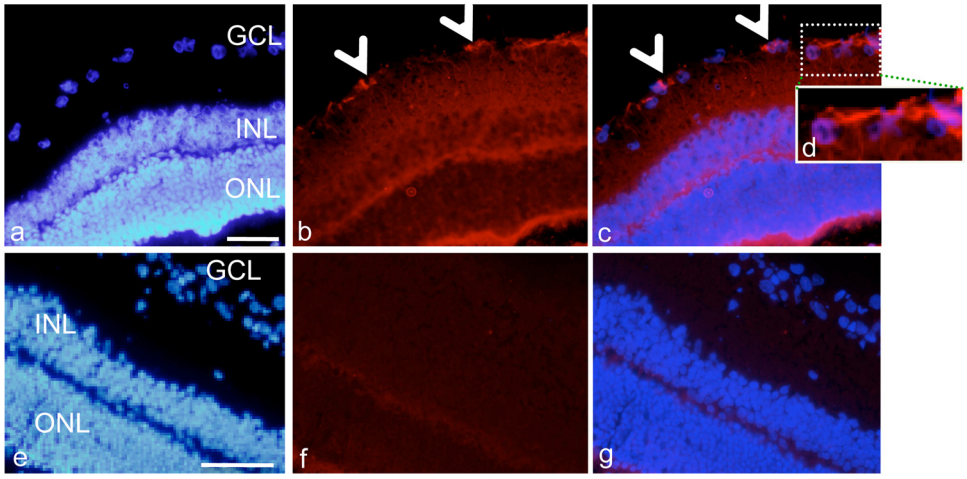


**FIG 4** Immunohistochemical analysis of the rat retina. Panels a to d show results 1 h after 5 instillations a day of 10 $\mu$g/ml AC-8 for 4 days and then a single instillation on day 4 (group 3). Panels e to g show results 1 h after 5 instillations a day of PBS for 4 days and then a single instillation on day 4 (vehicle; group 6). Panel d is a higher magnification of the dashed white square in panel c. The left panels show DAPI staining (blue), the middle panels show Alexa-labeled anti-human IgG antibody (red), and the right panels show the merged images. Arrowheads point to positively stained astrocytes. GCL, ganglion cell layer; INL, inner nuclear layer; ONL, outer nuclear layer. Bar, 100 $\mu$m.

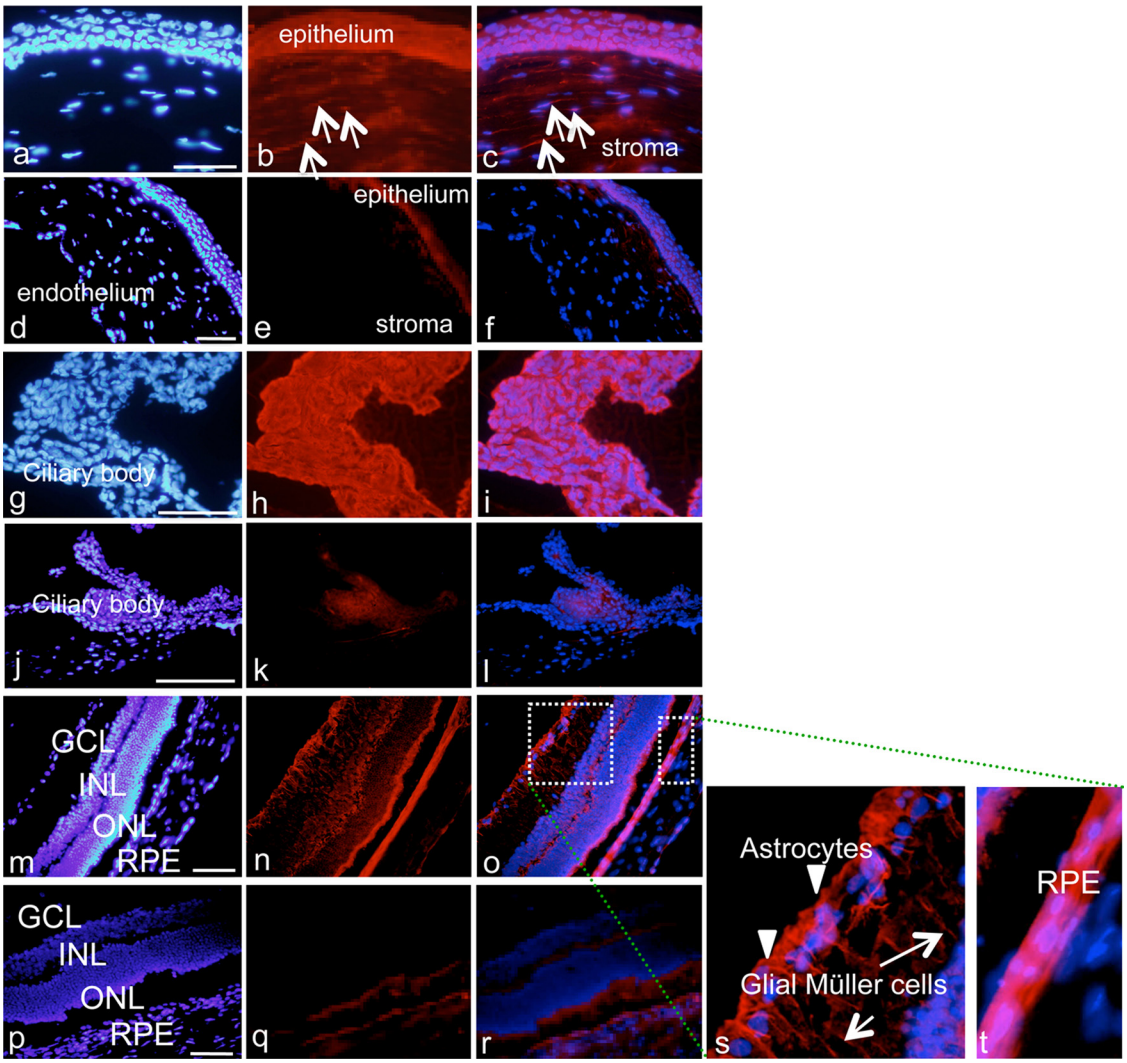


**FIG 5** Immunohistochemical analysis of the rat eye 1 h after one subconjunctival injection. Shown is cornea 1 h after one subconjunctival injection of 10 $\mu$g/ml AC-8 (group 4; a to c) or PBS (group 7; d to f). White arrows indicate positive anti-human IgG staining. Panels g to t show results for ciliary body (g to l) and retina (m to t) 1 h after subconjunctival injection of AC-8 (group 4; g to i, m to o, and s and t) or PBS (group 7, j to l and p to r). Panels s and t are two higher magnifications of the white dashed squares in panel o. In panel s, arrowheads indicate stained astrocytes in the inner part of the retina, and white arrows indicate stained Müller cell prolongations. The left column shows DAPI staining, the middle column shows Alexa-labeled anti-human IgG antibody, and the right column shows the merged images.

KOS virus was similar to that in the rat cornea (see Fig. S1 in the supplemental material).

**De-epithelialization did not change the distribution of AC-8 after subconjunctival injection.** Subconjunctival injection in eyes with central de-epithelialized corneas resulted in the same biodistribution of AC-8 as that observed after subconjunctival injection in normal eyes. Intense AC-8 staining was located in the peripheral cornea and in all ocular tissues of the anterior segment of the eye. Posterior segment penetration was not enhanced compared to that in non-de-epithelialized eyes (data not shown).

**Concentrations of AC-8 in ocular tissues and aqueous and vitreous humors.** In ocular tissues, the maximal concentration following topical treatment was found 1 h posttreatment in the corneal epithelium (18.7 ± 8 ng/mg) (mean ± standard deviation [SD]) and decreased rapidly thereafter (1.4 ± 0.5 ng/mg 6 h posttreatment). Interestingly the corneal stroma and endothelium had much lower concentrations of AC-8 (1.10 ± 1.09 ng/mg at 1 h and even at later time points), indicating that AC-8 does not move from the surface to the inner cornea. This suggests that AC-8 reaches the cornea mainly through the limbus and the sclera. In the aqueous humor, vitreous humor, retinas, and serum, levels of AC-8 were below the limit of quantification.

After subconjunctival injection, the AC-8 levels were significantly increased compared to after instillation, in all tested ocular tissues, the aqueous humor, and the vitreous humor. The maximal AC-8 concentration was measured in the corneal epithelium 1 h posttreatment (3,894 ± 2,350 ng/mg) and decreased to 197 ± 104 ng/mg 6 h posttreatment. The AC-8 concentration in aqueous humor 1 h posttreatment was 1,368 ± 1,041 ng/ml, and it decreased to 777 ± 346 ng/ml 6 h posttreatment. The concentration in the vitreous humor was also high 1 h posttreatment (917 ± 570 ng/ml) and decreased more rapidly (117 ± 55 ng/ml) 6 h post-

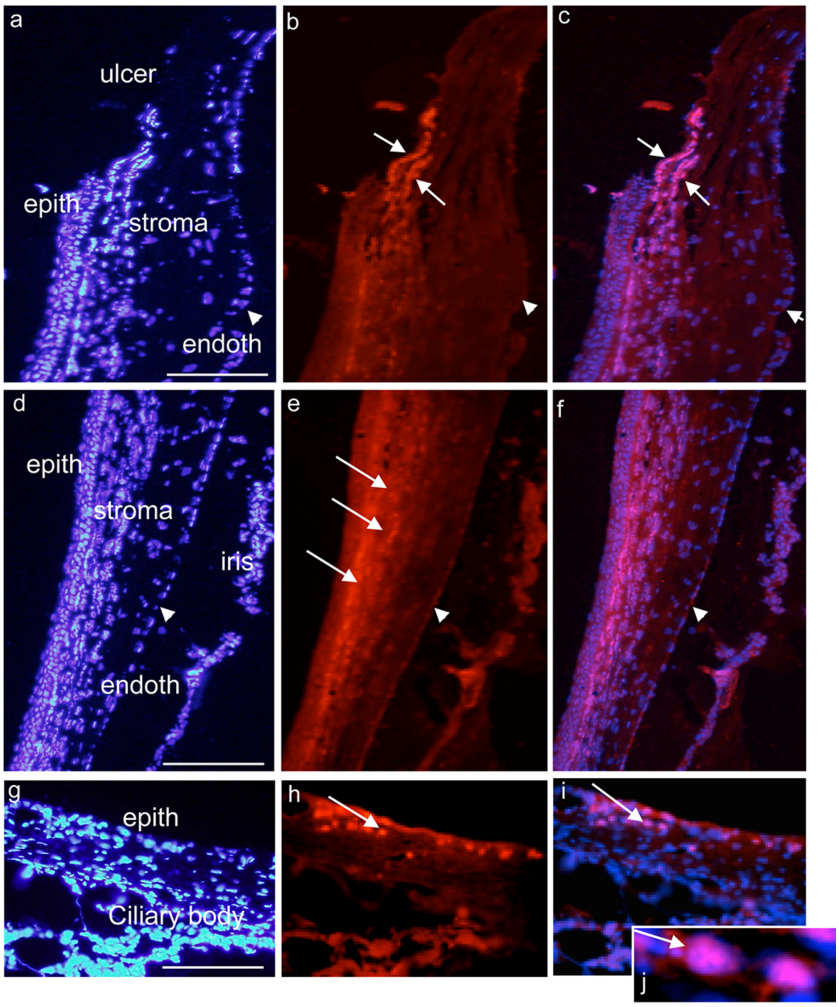


**FIG 6** Immunohistochemical analysis of the ulcered rat cornea 1 h after 5 hourly instillations of drops of 100 $\mu$g/ml AC-8 (group 1). Panels a to c show the junction between epithelialized and de-epithelialized corneal areas (central cornea). White arrows indicate positive AC-8 labeling, and arrowheads indicate corneal endothelium. In peripheral cornea and iris (d to f), white arrows indicate positive AC-8 labeling and arrowheads indicate corneal endothelium (very weak labeling). Panels g to j show IHC analysis of the limbus and ciliary body areas 24 h after 5 instillations of AC-8 (group 2). Panel j is a magnification of panel i. Panels h to j show positive AC-8 labeling in the subepithelial area (arrows). The left column shows DAPI staining, the middle column shows Alexa-labeled anti-human IgG antibody, and the right column shows the merged images. Bar, 200 $\mu$m.

treatment. The amount of AC-8 in the corneal epithelium was much higher after subconjunctival administration, suggesting a translimbal pathway. As was seen with topical administration, high concentrations of AC-8 were not achieved in the stroma and endothelium. The quantity of AC-8 was higher in the retina than after topical administration, but this did not correlate with the heterogeneous distribution of the molecule in peripheral versus central retinas. In the serum, AC-8 was detected but at a lower level than in ocular fluids (126 $\pm$ 59 ng/ml and 34 $\pm$ 11 ng/ml 1 and 6 h posttreatment, respectively), as expected.

**Spectrum of activity of AC-8 against a panel of ocular HSV isolates and laboratory strains.** AC-8 had previously been tested only against a limited number of laboratory strains, none of which were isolated from ocular infections (4). We therefore tested the activity of AC-8 against a panel of 11 low-passage ocular isolates and the laboratory strains KOS and F, using a yield reduction assay. Figure 8 demonstrates that there was a dose-dependent reduction in the yield of virus for all strains tested. Table 2 shows the calculated $MEC_{50}$ and $MEC_{90}$ values for each strain of virus. The $MEC_{50}$ values ranged from 0.01 to 0.04 $\mu$g/ml, and the $MEC_{90}$ values ranged from 0.04 to 0.13 $\mu$g/ml. Analysis of the data by Kruskal-Wallis ANOVA on ranks and Wilcoxon signed-rank test revealed none of these concentrations were significantly different. These results indicate that AC-8 has broad-spectrum activity.

***In vivo* efficacy of AC-8 against HSV-1 KOS. (i) Determination of $MEC_{50}$ and $MEC_{90}$ values of the formulated test articles.** Prior to dosing animals, the activity of the formulated test articles was tested using a yield reduction assay as described above. The $MEC_{50}$ and $MEC_{90}$ values for AC-8 were 0.030 and 0.085 $\mu$g/ml ($5.7 \times 10^{-10}$ and $1.6 \times 10^{-9}$ M), respectively, and those for TFT were 0.380 and 0.510 $\mu$g/ml ($1.3 \times 10^{-6}$ and $1.7 \times 10^{-6}$ M), respectively. The control Fab fragment had no effect on viral titers.

**(ii) Mean clinical disease scores.** Clinical scoring of the disease was performed after an 8-day treatment of HSV-1 KOS-infected mice. From day 0 (day of corneal viral inoculation) to day 8, mice were treated as follows: group 1, 1% trifluridine; group 2, 1 mg/ml

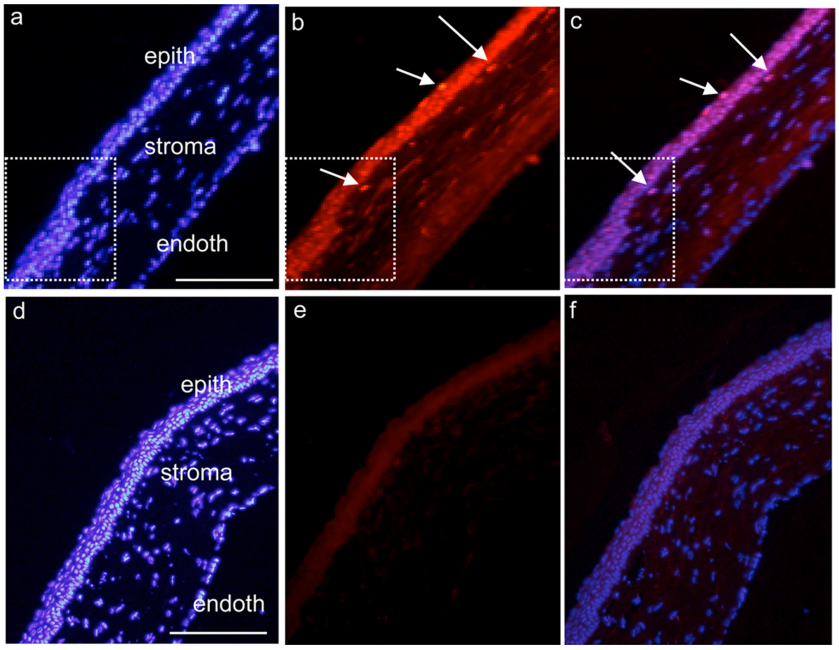


**FIG 7** Immunohistochemical analysis of the junction between epithelialized and re-epithelialized rat cornea 1 h after 5 instillations per day for 2 days and then 1 instillation on the last day of treatment with 100 $\mu$g/ml AC-8 (group 3; a, b, and c) or vehicle (group 7; d, e, and f). Positive AC-8 labeling is detected in the epithelium and in some subepithelial cells (b and c; arrows). White squares delineate the junction between intact and re-epithelialized areas (note irregular re-epithelialization). epith, epithelium; endoth, endothelium. The left column shows DAPI staining, the middle column shows Alexa-labeled anti-human IgG antibody, and the right column shows the merged images. Bar, 200 $\mu$m.

AC-8 in PBS; group 3, 10 mg/ml AC-8 in PBS; group 4, 10 mg/ml control Fab fragment in PBS; group 5, PBS (pH 7.0) vehicle. Mean disease scores for each parameter and group are shown in Fig. 9. Scores were evaluated from day 0 to day 15, although treatment was stopped at day 8. All groups developed blepharitis by day 1, and this continued to increase until day 7, when it peaked between 1.4 and 2.0 (Fig. 9A). Through day 7, none of the groups were significantly different. After day 7, blepharitis began to heal, and it appeared to heal faster in the TFT group (score at 0 on day 11 for TFT, day 13 for AC-8 low dose, and day 15 for AC-8 high dose). All groups had scores below 0.5 by the end of the study on day 15. Blepharitis scores in the TFT group were never more severe than a score of about 0.75. The fact that animals treated with 1 or 10 mg/ml AC-8, respectively, had lower disease scores at peak on day 7 or 9 suggests that it was having some effect. We observed that the PBS-treated eyes had one of the highest scores on day 7, but the severity decreased up to the end of the study. It is possible that the increased severity of inflammation in the control Fab-treated group may be due to the Fab fragment enhancing inflammatory responses. Statistical analysis showed that blepharitis scores were significantly different on day 9 for control Fab fragment versus TFT groups.

Corneal vascularization was delayed in all groups and did not appear until day 11 (Fig. 9B). Levels of corneal vascularization were similar in the AC-8 high-dose-treated group and the TFT-treated group. Vascularization scores ranged between 0.3 (TFT and high-dose AC-8) and 0.9 (low-dose AC-8 and Fab fragment) on day 15 and were not statistically different.

When epithelial keratitis was measured by fluorescein staining, there appeared to be one peak between days 3 and 5 and another one between days 9 and 11 (Fig. 9C). Typically, epithelial keratitis appears early and the cornea heals within 2 to 3 days, which would correspond with the peak on days 3 and 5. The latter peak is probably due to collateral damage from the stromal keratitis and from drying of the cornea, as the inflamed eyelids do not close properly. The TFT group had the smallest amount of epithelial staining. The PBS group had the largest amount of epithelial staining, with the low- and high-dose AC-8 groups falling in the middle. Statistical analysis showed that epithelial keratitis scores were significantly different on days 3 (PBS versus TFT) and 5 (PBS, Fab fragment, low- and high-dose AC-8 groups versus TFT group). Because AC-8 scores were essentially bracketed by the Fab fragment and TFT scores, they were not significantly different from those of the other groups.

For corneal opacity (Fig. 9D), TFT and AC-8 at 1 and 10 mg/ml are effective during the administration period (day 0 to day 8), with mean scores of less than 0.1. In both the low- and high-dose AC-8 groups, there was a delay in the onset of corneal opacity (score, $>$0.1): day 9 for the low dose and day 13 for the high dose. The low-dose AC-8 group reached a score of 0.9 on day 15, while the high-dose AC-8 and TFT groups reached a score of 0.6 on the same day. These results suggest that there was a dose-response effect. Mice in the PBS group had scores that were either higher or lower than those of both AC-8 groups, depending on the day. Opacity scores were not significantly different between any of the groups at any time.

**(iii) Percentage of mice with disease.** For blepharitis, 90 to 100% of the animals in all groups developed eyelid inflammation. With TFT treatment, 25% of mice failed to develop blepharitis on days 3 and 5. For vascularization, 30% of the mice developed corneal blood vessels. On day 15, the percentages ranged from 20% (TFT and high-dose AC-8) to 30% (low-dose AC-8 and con-

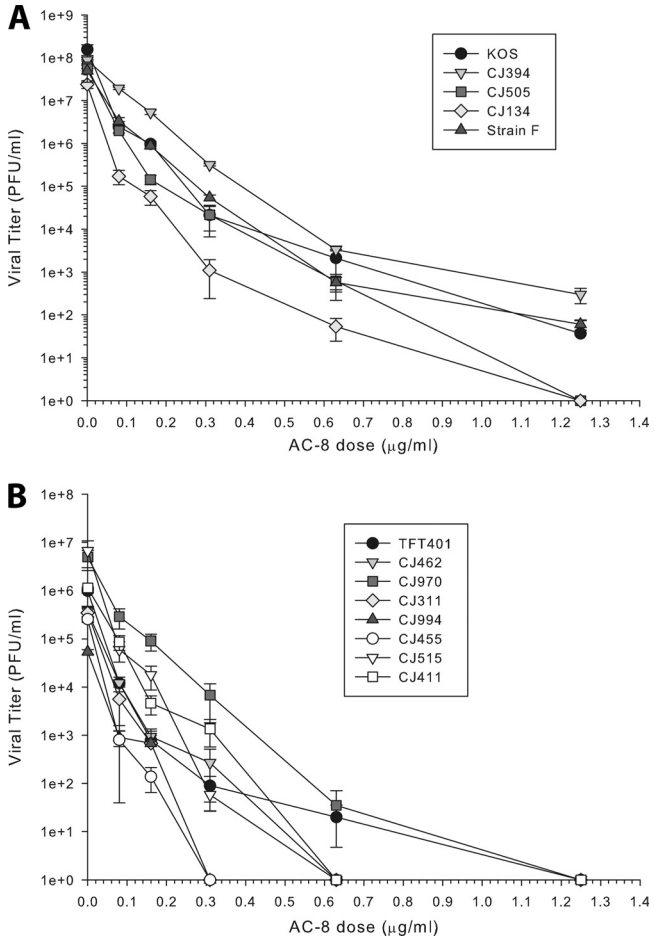


**FIG 8** Inhibition of ocular HSV-1 isolates by AC-8. Eleven low-passage clinical isolates (A and B) and the laboratory strains KOS and F (B) were tested. Virus was mixed with the desired concentration of AC-8 and then incubated with Vero cell monolayers (multiplicity of infection of 1.0) for 1 h at 37°C. The inoculums were removed. The cells were refed with medium containing AC-8 and incubated for 18 to 24 h. The cells were then lysed and clarified by centrifugation, and the virus titers of the supernatants were determined by plaque assay. The data points represent the means of triplicate samples ± standard errors of the means.

trol Fab fragment). The percentages for epithelial keratitis showed a curve similar to the mean disease scores. On day 3, the percentages of mice with epithelial keratitis were over 60% in the low- and high-dose AC-8 and Fab fragment groups, compared to the TFT group (30%). These data underscore the impression that Fab fragments are enhancing the disease.

The percentage data for corneal opacity paralleled the mean disease scores, with TFT reducing the number of mice with disease most effectively. A high dose of AC-8 was more effective than the low dose (90% versus 60% had no disease on days 9 and 11), and AC-8 delayed the onset of opacity by 4 to 6 days. The highest percentage of animals with disease (60%) was observed in the Fab fragment group, while the PBS group was either higher or lower than the AC-8 groups, depending on the study day.

**(iv) Tear film viral titers.** The TFT-treated group had negligible viral titers, not exceeding $1.3 \times 10^2$ PFU/ml on day 3 (Fig. 10). Among all other groups, the peak titer for the high-dose AC-8 group was the lowest at $5.8 \times 10^3$ PFU/ml on day 5. Viral titers peaked on day 3 for the Fab fragment-treated group and in all other groups on day 5. The PBS group had viral titers of $1.3 \times 10^4$ PFU/ml on day 5, which was between both AC-8 groups and the control Fab fragment group. These results suggest that the low-dose AC-8 treatment had a modest antiviral effect, compared to the high-dose AC-8 treatment and that the high-dose AC-8 treatment was less effective than the TFT treatment. As with the disease scores, both AC-8 groups were intermediate between the Fab fragment group (high titers and high disease scores) and the TFT group (low titers and low disease scores), which is consistent with a modest antiviral effect.

Statistical analysis of the titer data on day 1 showed that PBS group titers were significantly different from the ones in the TFT group. On days 3 and 5, PBS, Fab fragment, and low- and high-dose AC-8 group titers were significantly different from those in the TFT group. On day 7, the titers in the PBS and low-dose AC-8 groups were significantly different from those in the TFT group. Finally, the low-dose AC-8 group differed from the high-dose AC-8 group. When the groups were analyzed by taking their peak titers over time, the PBS, Fab fragment, and low- and high-dose AC-8 groups were significantly different from the TFT group ($P < 0.05$).

**(v) Histological analysis.** Histology revealed an all-or-nothing response in that there was significant inflammation and corneal edema in some eyes and little if any in others (10). The pathology was well correlated with the corneal opacity score for each mouse in that if the opacity score was low, there was little if any pathology, and if the opacity score was high, there was severe pathology. The principal difference between the groups was in the number of mice that had low scores. These findings are consistent with previous studies showing that mice either develop severe disease or little if any (10). For most of the parameters, we found there was little if any difference between the groups. Overall, the histological analysis was uninformative in terms of showing consistent differences between the treatment groups.

## DISCUSSION

Herpes keratitis remains the leading cause of corneal blindness due to infection in the industrialized nations, with over 500,000

**TABLE 2** $MEC_{50}$ and $MEC_{90}$ values for HSV strains obtained via the yield reduction assay

| Virus strain | MEC (μg/ml)[a] | |
|---|---|---|
| | 50% | 90% |
| CJ134 | 0.013 ± 0.003 | 0.042 ± 0.003 |
| CJ311 | 0.013 ± 0.007 | 0.045 ± 0.005 |
| CJ394 | 0.040 ± 0.000 | 0.130 ± 0.000 |
| CJ411 | 0.013 ± 0.007 | 0.060 ± 0.000 |
| CJ455 | 0.012 ± 0.002 | 0.035 ± 0.000 |
| CJ462 | 0.020 ± 0.005 | 0.058 ± 0.006 |
| CJ505 | 0.022 ± 0.002 | 0.053 ± 0.003 |
| CJ515 | 0.025 ± 0.010 | 0.048 ± 0.013 |
| CJ970 | 0.030 ± 0.015 | 0.088 ± 0.028 |
| CJ994 | 0.018 ± 0.002 | 0.045 ± 0.000 |
| TFT401 | 0.012 ± 0.002 | 0.047 ± 0.003 |
| KOS | 0.010 ± 0.010[b] | 0.050 ± 0.005 |
| F | 0.040 ± 0.030 | 0.103 ± 0.043 |

[a] 50% and 90%, $MEC_{50}$ and $MEC_{90}$, respectively. The measurements were performed in triplicate. Data are presented as means ± standard errors of the means.
[b] The molar equivalent for $MEC_{50}$ for KOS (0.01 μg/ml) is $1.88 \times 10^{-10}$ M.

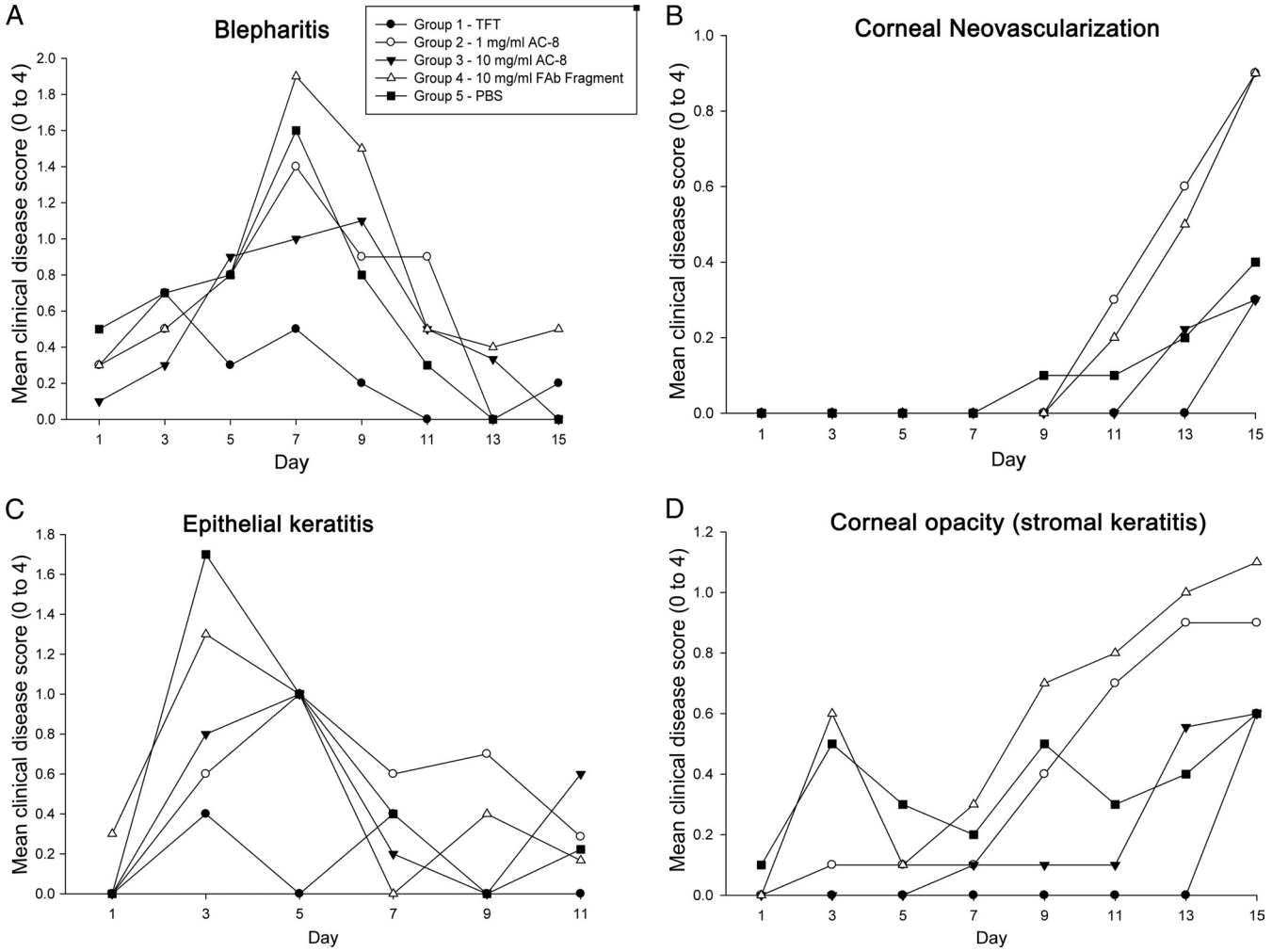


**FIG 9** Mean ocular disease scores of HSV-1 KOS-infected mice over the 15-day study period. Shown are mean disease scores for blepharitis (A), corneal neovascularization (B), epithelial keratitis (C), and corneal opacity (stromal keratitis) (D). The inset in panel A denotes the symbols for each group. The scoring scale (0 to 4) is described in Table 1. TFT, trifluridine.

affected in the United States (14). Antiviral drugs are available, but they have shown limited utility, and toxicity and viral resistance are still unanswered issues. Topical trifluridine (1%) given at 2-h intervals nine times daily is the treatment approved in the United States. As the dendrites begin to regress, the dosage is tapered until the lesion resolves completely (usually in 7 to 10 days). At this point, however, the patient must continue the medication for another week to ensure suppression of the virus. Monoclonal antibody therapy has an advantage as it can be applied topically without any preservative or enhancer, reducing the potential for subsequent surface irritation due to repeated instillation. Another advantage could be a reduced frequency of instillation if the Fab can penetrate epithelial cells and remain stable for several hours. In this study, we have shown that potentially therapeutic concentrations of AC-8 (10 to 40 ng/ml) were found in the corneal epithelium (9,057 ng/mg) after instillation. Twenty-four hours after instillation, most of the AC-8 was cleared from the ocular tissues. The fact that AC-8 was undetectable in the systemic compartment could be another advantage of ocular delivery.

Previous studies (12, 24) had shown that proteins or peptides

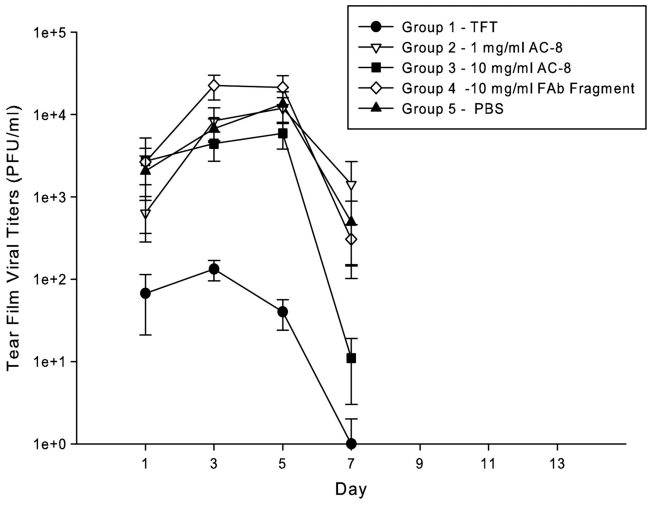


**FIG 10** Mean tear film viral titers. Tear film samples were collected from the HSV-1 KOS-infected mice at the indicated times, serially diluted, and quantified by plaque assay on Vero cell monolayers. The inset denotes the symbols representing each group. TFT, trifluridine. The data presented are means ± standard errors of the means.

of about 25 kDa could penetrate the eye following topical instillation. Consistent with Furrer et al. using a single-chain antibody (6), we observed that AC-8 (53 kDa) penetrated the cornea and other ocular tissues primarily via a limbal route. This was further confirmed by the fact that de-epithelialization of the cornea did not dramatically increase the intrastromal penetration of AC-8 at the site of epithelial damage.

Interestingly, in both the cornea and retina, AC-8 was found in ocular cells that engulfed the Fab fragment. In the normal cornea, AC-8 was mostly located in stromal cells and in subepithelial dendritiform cells that could correspond to Langerhans cells. This cellular uptake could explain the observation that AC-8 levels were much higher in the epithelium than in the stroma, where the cellular density is lower. In the retina, AC-8 was found in astrocytes and Müller cells, indicating a possible retinal biodistribution of a topically or subconjunctivally administered antibody.

In the newly formed epithelium, when AC-8 was instilled during the period of corneal epithelial healing, intraepithelial penetration was greater, suggesting that the uptake by epithelial cells could be enhanced by physiological changes in the cells associated with healing. This biodistribution cannot be extrapolated to the binding of AC-8 instilled on an HSV-1-infected cornea. In the latter case, AC-8 should bind preferentially to its specific target to neutralize HSV-1. It is important to note that AC-8 can remain in cells and provide protection. Additionally, HSV corneal infection is known to trigger the migration of dendritic cells into the central cornea, and these cells could serve as a reservoir for AC-8 (2).

The glial uptake of AC-8 was very similar to what is observed when bevacizumab (21) or VP22 (a protein from the tegument of HSV) was injected into the vitreous humor of rabbit or rat eyes (16). The transretinal movement of proteins from the vitreous humor is probably taking place, in part, through a glial pathway. As predicted, subconjunctival injection of AC-8 was much more efficient in delivering AC-8 to both the cornea and the other eye tissues than topical instillation (50- to 1,000-fold difference in AC-8 concentration). How drugs penetrate the eye by the subconjunctival route remains controversial (8). It is thought that several dynamic barriers are responsible for systemic drainage and limit intraocular penetration of compounds in tissues (8). However, we have previously shown that oligonucleotides were efficiently delivered to the cornea using subconjunctival injection (1), and the present study confirms that subconjunctival injection is also efficient in targeting the cornea using a 53-kDa protein. Other studies have shown that subconjunctival injections of bevacizumab inhibited corneal angiogenesis in different models (9, 17). High levels of bevacizumab were measured in the anterior and posterior segments of the rabbit eye by this route of administration (15).

When we compared the $MEC_{50}$ values for AC-8 with 11 low-passage clinical ocular isolates, as well as strains KOS and F, they ranged from 0.01 to 0.04 $\mu$g/ml. These values were not significantly different from each other, indicating that AC-8 has broad-spectrum activity against ocular strains of HSV. Considering the essential role of gD (the target of AC-8) in viral infection (22), this is not surprising. Previously, a $MEC_{50}$ value of 0.25 $\mu$g/ml was reported for a human Fab to gD using HSV-1 strain F (4), and our value was approximately 12-fold lower (0.02 $\mu$g/ml). It is not clear why these values differ, but it may be due to differences in the assays that were used. The $MEC_{50}$ was 10-fold higher with TFT than with AC-8, suggesting that, using higher doses of AC-8, a stronger *in vivo* efficacy would have been expected. However, the analysis of clinical parameters and tear film viral titers indicated that TFT was more effective than AC-8.

Trifluridine has been shown to induce mild toxic changes such as intracellular edema of the basal cell layer, mild thinning of the overlying epithelium, and reduced strength of stromal wounds (13). Consequently, continuous administration for periods exceeding 21 days is not recommended. This means that there is a need for less toxic molecules, and the efficacy/toxicity ratio of TFT could be weighed against that of AC-8, especially for long-term treatments.

Treatment with low-dose AC-8 (1 mg/ml) reduced ocular disease scores slightly. Treatment with high-dose AC-8 (10 mg/ml) achieved a greater reduction in clinical disease scores, but not as much as the treatment with TFT. Because the two AC-8 groups had scores intermediate between the negative and positive controls, the differences were not significant, although there was a dose response as an indication of efficacy. Viral titer data paralleled the disease data, with AC-8 reducing titers, but not as much as TFT. A determination of the $MEC_{50}$ values for the formulated test articles revealed they were active. In summary, AC-8 appears to have an effect, but it is not as strong as TFT. We did not attempt subconjunctival injection in the *in vivo* efficacy study because it would be less tolerable than topical delivery. However, if subconjunctival delivery resulted in a depot effect with prolonged release, this might be an advantage. Further studies are warranted.

Three factors are important in determining whether an antiviral agent may have clinical utility. First, the agent must be nontoxic. Our data indicated little or no inflammation or cellular damage was seen even after repeated doses of AC-8 were given. The second is that sufficient concentrations of AC-8 must be delivered to the target tissue and that therapeutic levels can be sustained. Our data indicate that AC-8 can be delivered to ocular tissues and can remain for several hours at therapeutic concentrations. The third factor is that the agent must have activity against a majority of viral strains. Our data showed that all 13 HSV strains were sensitive to AC-8 at $MEC_{50}$ values of 10 to 40 ng/ml. However, in an *in vivo* mouse model of herpes-induced keratitis, in spite of a clear indication that the amounts of HSV-1 are reduced in the tears following AC-8 treatment, clinical evaluation showed that additional studies to improve the *in vivo* efficacy of AC-8 would be needed for clinical utility.

## ACKNOWLEDGMENTS

This study was supported by ribOvax Biotechnologies, Geneva, Switzerland, and a Core Grant for Vision Research from the NIH to the University of Wisconsin—Madison (P30 EY016665).

We thank Robert Gurny and Cinzia Stella-Deutsch from the University of Geneva, Switzerland, for expertise in AC-8 solution preparation and conditioning.

## REFERENCES

1. **Andrieu-Soler C, et al.** 2005. Downregulation of IRS-1 expression causes inhibition of corneal angiogenesis. Invest. Ophthalmol. Vis. Sci. **46**:4072–4078.
2. **Asbell PA, Kamenar T.** 1987. The response of Langerhans cells in the cornea to herpetic keratitis. Curr. Eye Res. **6**:179–182.
3. **Brandt CR, Coakley LM, Grau DR.** 1992. A murine model of herpes simplex virus-induced ocular disease for antiviral drug testing. J. Virol. Methods **36**:209–222.
4. **Burioni R, Williamson RA, Sanna PP, Bloom FE, Burton DR.** 1994. Recombinant human FAb to glycoprotein D neutralizes infectivity and prevents cell-to-cell transmission of herpes simplex viruses 1 and 2 in vitro. Proc. Natl. Acad. Sci. U. S. A. **91**:355–359.

5. **De Logu A, et al.** 1998. Characterization of a type-common human recombinant monoclonal antibody to herpes simplex virus with high therapeutic potential. J. Clin. Microbiol. **36**:3198–3204.
6. **Furrer E, et al.** 2009. Pharmacokinetics and posterior segment biodistribution of ESBA105, an anti-TNF-alpha single-chain antibody, upon topical administration to the rabbit eye. Invest. Ophthalmol. Vis. Sci. **50**:771–778.
7. **Grau DR, Visalli RJ, Brandt CR.** 1989. Herpes simplex virus stromal keratitis is not titer-dependent and does not correlate with neurovirulence. Invest. Ophthalmol. Vis Sci. **30**:2474–2480.
8. **Kim SH, Lutz RJ, Wang NS, Robinson MR.** 2007. Transport barriers in transscleral drug delivery for retinal diseases. Ophthalmic Res. **39**:244–254.
9. **Kim TI, Kim SW, Kim S, Kim T, Kim EK.** 2008. Inhibition of experimental corneal neovascularization by using subconjunctival injection of bevacizumab (Avastin). Cornea **27**:349–352.
10. **Kintner RL, Brandt CR.** 1995. The effect of viral inoculum level and host age on disease incidence, disease severity, and mortality in a murine model of ocular HSV-1 infection. Curr. Eye Res. **14**:145–152.
11. **Koevary SB, Nussey J, Lake S.** 2002. Accumulation of topically applied porcine insulin in the retina and optic nerve in normal and diabetic rats. Invest. Ophthalmol. Vis. Sci. **43**:797–804.
12. **Lambiase A, Tirassa P, Micera A, Aloe L, Bonini S.** 2005. Pharmacokinetics of conjunctivally applied nerve growth factor in the retina and optic nerve of adult rats. Invest. Ophthalmol. Vis. Sci. **46**:3800–3806.
13. **Lass JH, Langston RH, Foster CS, Pavan-Langston D.** 1984. Antiviral medications and corneal wound healing. Antiviral Res. **4**:143–157.
14. **Liesegang TJ.** 2001. Herpes simplex virus epidemiology and ocular importance. Cornea **20**:1–13.
15. **Nomoto H, et al.** 2009. Pharmacokinetics of bevacizumab after topical, subconjunctival, and intravitreal administration in rabbits. Invest. Ophthalmol. Vis. Sci. **50**:4807–4813.
16. **Normand N, et al.** 2005. VP22 light controlled delivery of oligonucleotides to ocular cells in vitro and in vivo. Mol. Vis. **11**:184–191.
17. **Papathanassiou M, et al.** 2008. Inhibition of corneal neovascularization by subconjunctival bevacizumab in an animal model. Am. J. Ophthalmol. **145**:424–431.
18. **Rodrigues EB, et al.** 2009. Therapeutic monoclonal antibodies in ophthalmology. Prog. Retin Eye Res. **28**:117–144.
19. **Sanna PP, et al.** 1996. Protection of nude mice by passive immunization with a type-common human recombinant monoclonal antibody against HSV. Virology **215**:101–106.
20. **Sanna PP, Deerinck TJ, Ellisman MH.** 1999. Localization of a passively transferred human recombinant monoclonal antibody to herpes simplex virus glycoprotein D to infected nerve fibers and sensory neurons in vivo. J. Virol. **73**:8817–8823.
21. **Shahar J, et al.** 2006. Electrophysiologic and retinal penetration studies following intravitreal injection of bevacizumab (Avastin). Retina **26**:262–269.
22. **Spear PG, Longnecker R.** 2003. Herpesvirus entry: an update. J. Virol. **77**:10179–10185.
23. **Visalli RJ, Brandt CR.** 1993. The HSV-1 UL45 18 kDa gene product is a true late protein and a component of the virion. Virus Res. **29**:167–178.
24. **Williams KA, et al.** 2005. Topically applied antibody fragments penetrate into the back of the rabbit eye. Eye (Lond.) **19**:910–913.
25. **Zeitlin L, et al.** 1998. A humanized monoclonal antibody produced in transgenic plants for immunoprotection of the vagina against genital herpes. Nat. Biotechnol. **16**:1361–1364.
26. **Zeitlin L, et al.** 1996. Topically applied human recombinant monoclonal IgG1 antibody and its FAb and F(ab′)2 fragments protect mice from vaginal transmission of HSV-2. Virology **225**:213–215.